New Journal of Physics
The open-access journal for physics

Electromagnetic wave focusing from sources inside a two-dimensional left-handed material superlens

Koray Aydin[1,2,4], **Irfan Bulu**[1,2] **and Ekmel Ozbay**[1,2,3]

[1] Nanotechnology Research Center, Bilkent University, Bilkent, 06800 Ankara, Turkey
[2] Department of Physics, Bilkent University, Bilkent, 06800 Ankara, Turkey
[3] Department of Electrical and Electronical Engineering, Bilkent University, Bilkent, 06800 Ankara, Turkey
E-mail: aydin@fen.bilkent.edu.tr

New Journal of Physics **8** (2006) 221
Received 26 June 2006
Published 3 October 2006
Online at http://www.njp.org/
doi:10.1088/1367-2630/8/10/221

Abstract. Lenses made of negative index materials exhibit different focusing behaviours compared to positive index material lenses. Flat lens behaviour and imaging below the diffraction limit is possible with negative refractive index lenses. In this study, we employed left-handed materials (LHM) as negative index materials and experimentally investigated the focusing behaviour of such lenses. A point source is embedded inside the LHM lens. We have shown that it is possible to focus electromagnetic (EM) waves by using a planar configuration of lenses that is constructed by using two-dimensional (2D) LHMs. Flat lens behaviour is observed at 3.89 GHz, where EM waves are focused along the lateral and longitudinal directions. At 3.77 GHz, where the reflection is measured to be minimum, the focusing effect occurred at the surface of the LHM with a spot size of 0.16λ. We were able to overcome the diffraction limit with a slab-shaped LHM superlens.

[4] Author to whom any correspondence should be addressed.

PII: S1367-2630(06)27440-8

Contents

1. Introduction

Artificially structured materials with negative values of permittivity (ε) and permeability (μ) are candidates for constructing left-handed materials (LHM) with an effective negative refractive index. The left-handed media phenomenon was brought to the attention of the scientific community by Veselago four decades ago [1], and has received great attention in recent years, since the first experimental demonstration of LHMs by Smith *et al* [2]. The experimental realization of LHMs became possible after the proposal of split-ring resonator (SRR) structures for obtaining negative permeability values by Pendry *et al* [3]. To achieve left-handed behaviour, one should combine SRR arrays together with thin wire arrays providing in turn negative permittivity [4]. At the frequency region covering both the negative values of ε and μ, the metamaterial will possess negative values of refractive index. We have successfully proposed a method to identify the true left-handed behavior [5], and recently studied the effect of disorders on the LHMs' transmission characteristics [6]. Besides the characterization of LHMs in terms of their transmission properties, Shelby *et al* were the first to demonstrate the negative refractive index of LHMs experimentally [7]. Further experimental studies using wedge-shaped LHMs [8]–[10], employing negative phase velocity to calculate the negative refractive index [10] and measuring negative beam shift from the surface of the LHM slab [11] supported the existence of negative refraction.

Ordinary materials with a positive refractive index always require curved surfaces to focus EM waves. However, a parallel-sided slab lens constructed from a negative index material brings EM waves into focus [1, 12]. Double focusing occurs inside and outside the lens, which is easily deducible from a simple ray diagram. Such lenses are also called flat lenses because their surfaces are not curved. Negative index materials can restore the amplitude of evanescent waves and therefore enable subwavelength focusing [12]. The subwavelength imaging effect is demonstrated for photonic crystal structures [13, 14] and left-handed transmission-line lenses at the frequency regions where the refractive index is negative [15, 16]. Imaging properties of negative index superlenses have been investigated theoretically by several researchers [17]–[26]. Recently, subwavelength focusing in LHM structures employing commonly used SRR-wire geometry have been reported [27, 28]. Most of the experimental studies are performed in the microwave frequency regime, but recently subwavelength imaging at optical [29] and mid-infrared [30] frequencies have been successfully shown. Lenses made of materials with negative refractive indices may not necessarily cause subwavelength imaging [31]–[37]. Since the high-resolution details are present near the object, the position of the focal point is important for

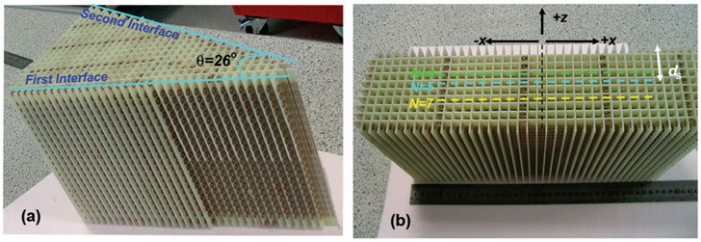

Figure 1. The pictures shown above are of 2D (a) wedge-shaped LHM with $\theta = 26^\circ$, (b) LHM slab lens with 10 unit cells along the propagation direction (z-axis).

observing subwavelength imaging. Although the subwavelength imaging is subject to restrictions and limitations, flat lens behaviour is present for all negative refractive index materials [38].

In this paper, we present our recent results on negative refraction and the focusing properties of LHMs. First, the negative index of refraction is verified by using a two-dimensional (2D) wedge shaped LHM. Subsequently, we investigated the focusing properties of a flat lens with the omni-directional sources that were embedded inside the lens. We observed a clear image of the source at 3.89 GHz. The electromagnetic (EM) waves are focused along the longitudinal and lateral directions at this frequency. The measured reflection spectrum of 2D LHM provides a dip at 3.77 GHz. At this special frequency, the image forms at the surface of the LHM lens with considerably higher subwavelength features (0.16λ).

2. Negative refraction

In the following section, we provide the experimental results on the focusing properties of LHMs. Before we commence the experimental analysis of the focusing properties, we wanted to verify that the 2D LHM lens possesses negative refractive index values at the frequencies where left-handed behaviour is observed [10]. In both refraction and focusing experiments, we used 2D LHM structures with the parameters provided in [10]. SRR arrays and wire arrays are arranged as interlocking units so that the resulting composite metamaterial responds to the incident EM wave in two dimensions.

Wedge-shaped structures are commonly used in order to measure the refractive index of LHMs, which is a typical experimental method for the observation of left-handed properties [7]–[10]. We constructed a wedge-shaped LHM with a wedge angle of $\theta = 26^\circ$ as seen in figure 1(a). The first interface of LHM is excited with EM waves emerging from the source located at a distance of 13 cm ($\sim 2\lambda$) away from the first interface of the wedge. The receiver antenna is mounted on a rotating arm to obtain the angular distribution of the transmitted signal, which is placed 70 cm ($\sim 10\lambda$) away from the second interface of the wedge. The angular refraction spectrum is scanned by $\Delta\theta = 2.5^\circ$ steps. The transmitter and receiver antennas are standard high gain microwave horn antennas that are connected to the HP 8510 C network analyser.

The refracted beam profiles from the LHM–air interface are shown in figure 2 for two different frequencies. Evidently, the transmitted beam is refracted on the negative side of the normal. The angle of the refraction at 3.77 GHz is measured to be $\theta_r = -65^\circ$ and at 3.89 GHz θ_r is -57.5°. Snell's law can be used to calculate the effective refractive index of the 2D LHM structure by the simple formula $n_{\text{eff}} \sin\theta_i = n_{\text{air}} \sin\theta_r$. At 3.89 GHz the refractive index is calculated to

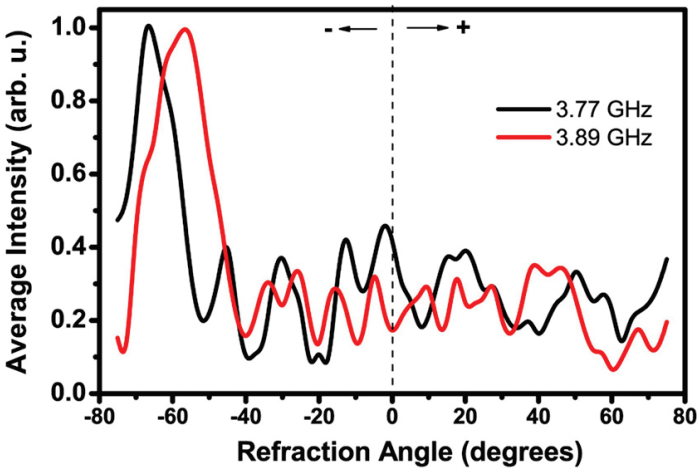

Figure 2. The refracted beam profiles at frequencies 3.77 (black) and 3.89 GHz (red).

be $n_{\text{eff}} = -1.92 \pm 0.05$. The angle of refraction increases when the frequency is lowered, hence the n_{eff} increases. The calculated refractive index at 3.77 GHz is $n_{\text{eff}} = -2.07 \pm 0.05$.

3. Focusing of EM waves

The presence of negative refraction enables the possibility for the slab structure to act like a lens for an omni-directional source. EM waves emerging from an omni-directional source that are located near such a lens will first be refracted through the first air–LHM interface and will come into focus inside the material. Then, outgoing EM waves will face refraction again at the second LHM–air interface and the refracted beam will meet the optical axis of a flat lens, where the second focusing will occur. However, for a parallel-sided slab lens that is made of positive refractive index material, EM waves will diverge, and thus cannot be focused. We have recently observed flat lens behaviour from the sources located outside of the LHM lens. In this study, we investigated the focusing behaviour of a flat lens where the omni-directional source is embedded inside the LHM slab. The focusing behaviour was previously observed inside LHM lenses experimentally [31]. We followed a different approach here. We chose to put the source inside the LHM lens and measure the field intensity outside the lens. This section is divided into two subsections. We first shall discuss the flat lens behaviour, where the lens focuses the incident EM wave in the lateral and longitudinal directions. Secondly, we will present our experimental observation of subwavelength imaging (superlens behaviour) near the LHM lens at the frequency where the LHM sample has the lowest reflection value.

In the focusing experiments a slab-shaped LHM lens with $40 \times 20 \times 10$ layers along the x, y and z directions is used. The top-view of the LHM lens is provided in figure 1(b). Along the propagation direction (z direction) the structure has 10 unit cells, in which the thickness is $t = 90.9$ mm. The periodicity along the z-direction, as well as along the x and y directions is $a_z = a_x = a_y = 9.3$ mm. We used monopole antennas as the point source. The monopole antenna was constructed by removing the shield around one end of a microwave coaxial cable. The exposed centre conductor, which also acted as the transmitter and receiver, was 3.8 mm long. This length is on the order of $\lambda/2$, arranged to work at a frequency range where left-handed

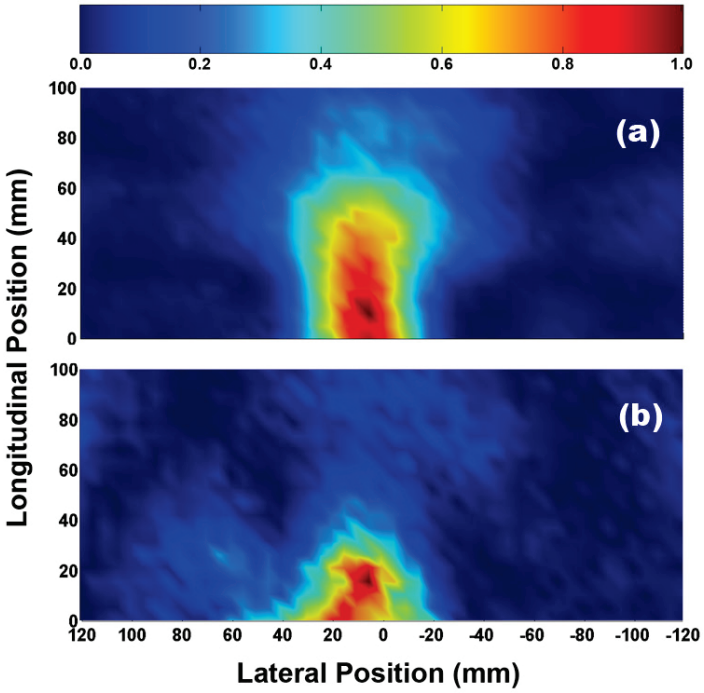

Figure 3. The spatial intensity distribution of the outgoing EM waves from the sources located inside the (a) fifth layer and (b) seventh layer of the LHM slab lens at 3.89 GHz.

behaviour was observed. We embedded the source inside the LHM lens at different locations. We chose routinely to identify the position of the source in terms of the number of layers (N_s). In figure 1(b) coloured dashed lines show the axis of the sources, which is d_s away from the LHM–air surface. The distance of the source to the LHM–air interface can be given by the formula $d_s = 9.3(N_s - 1) + r$, where $r = 3.6$ mm is the radius of the SRR. The intensity distribution of an EM wave is scanned from the surface by another monopole antenna with $\Delta x = \Delta z = 2.5$ mm steps. In the experiments, we can solely measure EM field intensity at a point.

3.1. Flat lens behaviour

Figure 3 depicts the spatial intensity distribution of the outgoing EM waves from the sources embedded inside the layers $N_s = 5$ and $N_s = 7$ at 3.89 GHz. The intensities are normalized with respect to the maximum intensity values. For both cases, we observed focusing along the longitudinal and lateral directions. However, there is a change at the focal point, when the location of the source is changed. The EM waves are focused at $z = 10$ and 15 mm for the sources at the fifth and seventh layers. As the point source is moved away from the LHM–air surface, the focal length is increased, which is consistent with the imaging theory.

The spot sizes of the focused beams along the lateral direction (x) for both source distances are approx. 0.4λ. We were able to focus EM waves that were smaller than half of the wavelength. However, the distances of the focal point are away from the surface of the LHM lens. The FWHM of the focused beam will be smaller if the image is formed closer to the LHM lens, since the evanescent modes are present near the LHM lens.

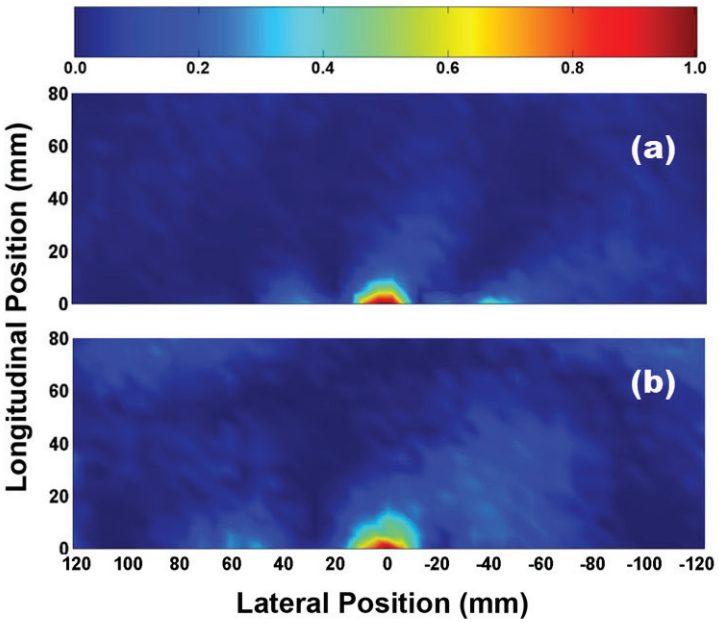

Figure 4. The spatial intensity distribution of the outgoing EM waves from the sources located inside the (a) fourth layer and (b) fifth layer of the LHM slab lens at 3.77 GHz.

3.2. Superlens behaviour

In the previous section, we investigated the imaging properties of the flat lens at 3.89 GHz. At a lower frequency, however, at $f = 3.77$ GHz, the imaging behaviour changes. Figure 4 displays the intensity distribution of the EM waves at 3.77 GHz where the sources are located inside the fourth and fifth layers of the LHM flat lens. The EM waves are focused along the lateral direction for both source distances. The imaging occurs near the LHM lens with subwavelength spot sizes. Similar experimental results were reported for photonic crystal lenses by Cubukcu *et al* [14].

We also performed scanning measurements in air by removing the LHM lens. The EM waves are scanned from 50 mm away from the point source. The resulting intensity distribution of the EM waves propagating in free space is provided in figure 5. The beam size in free space is clearly larger than that of the EM wave propagating inside the lens. We plotted the intensity profiles of the outgoing EM waves at $z = 0$ point for free space and LHM lens in figure 6. When the EM wave propagates 50 mm away from the source in free space (blue line), the full width at half maximum (FWHM) of the beam is measured to be 85 mm (1.07λ). FWHMs of the focused beam from the sources located inside the fourth and fifth layer of the LHM lens are 12.5 mm (0.16λ) and 17.5 mm (0.22λ), respectively. The intensities are normalized with the highest peak value for the source located inside the fourth layer, fifth layer and in air. The intensity of the beam travelling in air is multiplied by 0.5 in the figure. The highest transmission is observed in free space as expected. Intuitively, the transmission is higher for the source located in the fourth layer, since the EM waves travel less in the lossy LHM media.

Figure 7 depicts the intensity profiles of the EM waves near the LHM lens as a function of the frequency. In addition, the measured reflection spectra for the LHM slab are shown in figure 7 as a white line. As clearly seen in the figure, the minimum spot size is achieved at

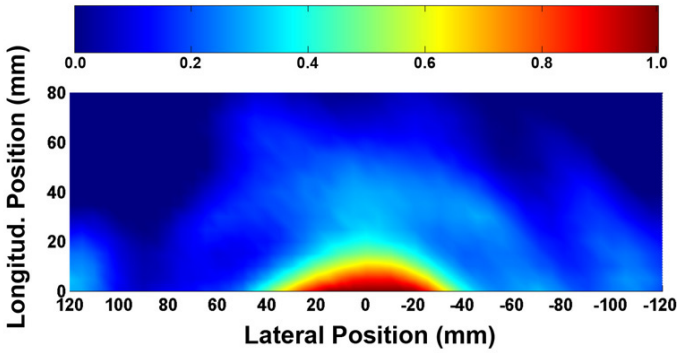

Figure 5. The spatial intensity distribution of the outgoing EM waves in free space from the source located at 50 mm away from the $z = 0$ point at 3.77 GHz.

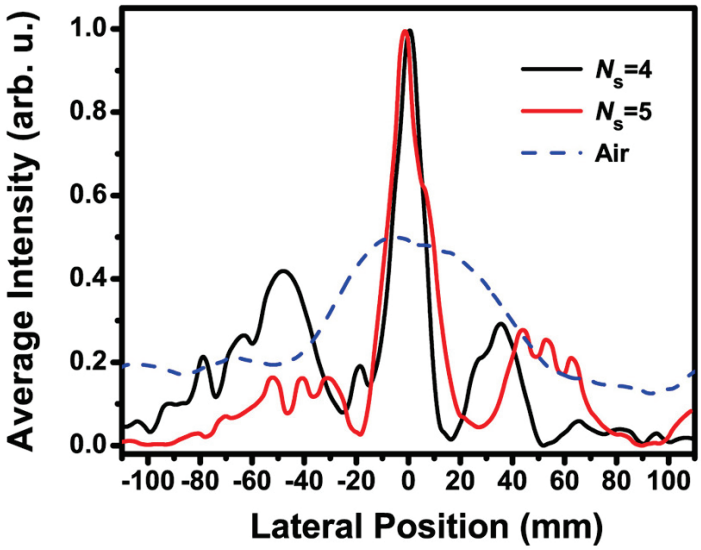

Figure 6. The focused beam profile near the LHM–air interface for the sources located inside the fourth layer (black) and fifth layer (red) of the LHM slab at 3.77 GHz. The blue dashed line represents the beam profile when the LHM lens is removed and EM waves propagate in air.

frequencies where the reflection is at a minimum. In recent study, we verified the impedance of the LHM to be matched to the free-space impedance at 3.77 GHz, where the reflection is very low [39]. Therefore, the losses due to the reflection do not significantly affect the resolution at this frequency. It is clear from figure 7 that the beam size of the EM waves at $z = 0$ point is at a minimum at 3.77 GHz. The beam size increases with an increase in the reflection value. To our knowledge this experiment is the first to have shown the effect of reflection on subwavelength imaging of LHM superlenses.

Pendry introduced the term perfect lens, a lens that is capable of overcoming the diffraction limit provided that $\varepsilon = \mu = -1$. However, it is not easy to fabricate a lossless and perfectly matched negative refractive index material. A perfect lens has not yet been experimentally shown; however it is possible to focus EM waves smaller than a half-wavelength size, which is

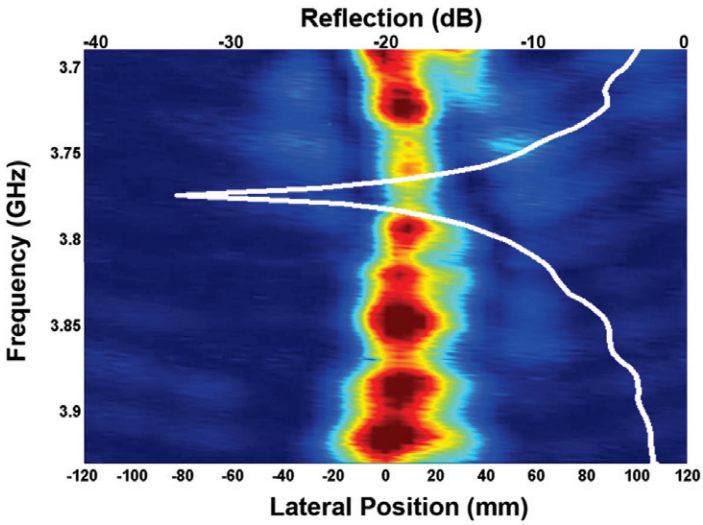

Figure 7. The intensity profiles of EM waves near the LHM lens as a function of frequency. The reflection spectrum of the LHM lens is shown in the figure with a white line.

the diffraction limit. The limitations on the subwavelength imaging are discussed for a perfect lens and deviations of material parameters from the ideal values have been shown to affect the subwavelength focusing [18]–[23]. The constructed image in our case is imperfect due to material losses and deviations from the ideal material parameters. The effective index of refraction -1.92 is quite different from the ideal refractive index $n = -1$. Nevertheless, small deviations from ideal parameters can be permitted to achieve subwavelength imaging [19]. It is theoretically shown that with the greater thickness of slab lens, superresolution reduces [19]. Our experimental results provided in figure 6, agree with this theoretical prediction, since the spot size increases when the source is located at a larger distance. This in turn means that the thickness of the superlens is increased.

Negative index materials can recover the evanescent modes in an image, which is not possible for a positive index material. These decaying modes carry information approximately at the near-field of the image. Evanescent modes are amplified at the surface of the LHM lens, in which these modes decay in free space. Evidently, the near-field information will be lost. Therefore, the focal point is important for resolving power of a superlens. At 3.77 GHz, we observed a spot size of 0.16λ, however at 3.89 GHz at the focal point, the spot size was 0.4λ. To our knowledge, our group is the first to demonstrate the effect of focal point on the spot size of the focused beam in subwavelength imaging.

4. Conclusion

In conclusion, we investigated the focusing characteristics of a flat LHM lens. The source is placed inside the LHM slab, in which flat lens behaviour is observed at 3.89 GHz. The EM wave is focused along the lateral and longitudinal directions at this frequency. However, at a lower frequency, 3.77 GHz, the focusing of EM waves occurred at the LHM–air surface. We achieved a 0.16λ spot size of the focused beam, which is well below the diffraction limit. The reflection

is minimum at 3.77 GHz, therefore the losses due to the reflection degrading the subwavelength imaging is reduced and higher subwavelength features can be resolved. It is not possible to obtain focusing from the sources inside lenses that are made of positive refractive index materials. The EM wave will diverge and never come into focus for a positive index planar lens. Materials with negative refractive indices can be ideal for lensing applications since they offer intriguing focusing behaviour that is unattainable from ordinary lenses. The surface impedance is nearly matched for LHM lenses, and planar configurations were able to be used. The main problem is to manufacture an ideal perfect lens. Currently, left-handed metamaterials are made of lossy substrates. Moreover, these structures absorb the EM waves that degrade the resolution limit. Meticulous designs are needed to achieve higher resolutions from negative refractive index superlenses.

Acknowledgments

This study is supported by the European Union under the projects EU-DALHM, EU-NOE-METAMORPHOSE, EU-NOE-PHOREMOST and TUBITAK under Project No. 104E090. One of the authors (EO) also acknowledges partial support from the Turkish Academy of Sciences.

References

[1] Veselago V G 1968 The elctrodynamics of substances with simultaneously negative values of permittivity and permeability *Sov. Phys. Usp.* **10** 504
[2] Smith D R, Padilla W J, Vier D C, Nemat-Nasser S C and Schultz S 2000 Composite medium with simultaneously negative permeability and permittivity *Phys. Rev. Lett.* **84** 4184–7
[3] Pendry J B, Holden A J, Robbins D J and Stewart W J 1999 Magnetism from conductors and enhanced nonlinear phenomena *IEEE Trans. Microwave Theory Tech.* **47** 2075–84
[4] Pendry J B, Holden A J, Robbins D J and Stewart W J 1998 Low frequency plasmons in thin-wire structures *J. Phys.: Condens. Matter* **10** 4785–809
[5] Aydin K, Guven K, Kafesaki M, Zhang L, Soukoulis C M and Ozbay E 2004 Experimental observation of true left-handed transmission peak in metamaterials *Opt. Lett.* **29** 2623–5
[6] Aydin K, Guven K, Katsarakis N, Soukoulis C M and Ozbay E 2004 Effect of disorder on magnetic resonance band gap of split-ring resonator structures *Opt. Exp.* **12** 5896–901
[7] Shelby R A, Smith D R and Schultz S 2001 Experimental verification of a negative *Science* **292** 77–9
[8] Parazzoli C G, Greegor R B, Li K, Koltenbah B E and Tanielian M 2003 Experimental verification and simulation of negative index of refraction using Snell's law *Phys. Rev. Lett.* **90** 107401
[9] Houck A A, Brock J B and Chuang I L 2003 Experimental observations of a left-handed material that obeys Snell's law *Phys. Rev. Lett.* **90** 137401
[10] Aydin K, Guven K, Soukoulis C M and Ozbay E 2005 Observation of negative refraction and negative phase velocity in left-handed metamaterials *Appl. Phys. Lett.* **86** 124102
[11] Aydin K and Ozbay E 2006 Negative refraction through impedance matched left-handed metamaterial slab *J. Opt. Soc. Am. B* **23** 415–8
[12] Pendry J B 2000 Negative refraction makes a lens *Phys. Rev. Lett.* **85** 3966–9
[13] Luo C, Johnson S G, Joannopoulos J D and Pendry J B 2003 Subwavelength imaging in photonic crystals *Phys. Rev. B* **68** 045115
[14] Cubukcu E, Aydin K, Ozbay E, Foteinopolou S and Soukoulis C M 2003 Subwavelength resolution in a two-dimensional photonic-crystal-based superlens *Phys. Rev. Lett.* **91** 207401

[15] Grbic A and Eleftheriades G V 2003 Subwavelength focusing using a negative-refractive-index transmission line lens *IEEE Antennas and Wireless Propagation Lett.* **2** 186–9
[16] Grbic A and Eleftheriades G V 2004 Overcoming the diffraction limit with a planar left-handed transmission-line lens *Phys. Rev. Lett.* **92** 117403
[17] Pendry J B and Ramakrishna S A 2003 Focusing light using negative refraction *J. Phys: Condens. Matter* **15** 6345–64
[18] Smith D R, Schurig D, Rosenbluth M, Schultz S, Ramakrishna S A and Pendry J B 2003 Limitations on subdiffraction imaging with a negative refractive index slab *Appl. Phys. Lett.* **82** 1506–8
[19] Fang N and Zhang X 2003 Imaging properties of a metamaterial superlens *Appl. Phys. Lett.* **82** 16161–3
[20] Lagarkov A N and Kissel V N 2004 Near-perfect imaging in a focusing system based on a left-handed-material plate *Phys. Rev. Lett.* **92** 077401
[21] Cummer S A 2003 Simulated casual subwavelength focusing by a negative refractive index slab *Appl. Phys. Lett.* **82** 1503–5
[22] Rao X S and Ong C K 2003 Subwavelength imaging by a left-handed material superlens *Phys. Rev. E* **68** 067601
[23] Chen L, He S and Shen L 2004 Finite-size effects of a left-handed material slab on the image quality *Phys. Rev. Lett.* **92** 107404
[24] Gomez-Santos G 2003 Universal features of the time evolution of evanescent modes in a left-handed perfect lens *Phys. Rev. Lett.* **90** 077401
[25] Feise M W and Kivshar Y S 2005 Sub-wavelength imaging with a left-handed material flat lens *Phys. Lett. A* **334** 326–30
[26] Zharov A A, Zharova N A, Shadrivov I V and Kivshar Y S 2005 Subwavelength imaging with opaque nonlinear left-handed lenses *Appl. Phys. Lett.* **87** 091194
[27] Aydin K, Bulu I and Ozbay E 2005 Focusing of electromagnetic waves by a left-handed metamaterial flat lens *Opt. Exp.* **13** 8753–9
[28] Bulu I, Caglayan H and Ozbay E 2006 Experimental demonstration of subwavelength focusing of electromagnetic waves by labyrinth-based two-dimensional metamaterials *Opt. Lett.* **31** 814–6
[29] Fang N, Lee H, Sun C and Zhang X 2005 Sub-diffraction limited optical imaging with a silver superlens *Science* **308** 534–7
[30] Korobkin D, Urzhumov Y and Shvets G 2006 Enhanced near-field resolution in midinfrared using metamaterials *J. Opt. Soc. Am. B* **23** 468–78
[31] Loschialpo P F, Smith D L, Forester D W, Rachford F J and Schelleng J 2003 Electromagnetics waves focused by a negative-index planar lens *Phys. Rev. E* **67** 025602
[32] Parazzoli C G, Greegor R B, Nielsen J A, Thompson M A, Li K, Vetter A M, Tanielian M H and Vier D C 2004 Performance of a negative index of refraction lens *Appl. Phys. Lett.* **84** 3232–4
[33] Brock J B, Houck A A and Chuang I L 2004 Focusing inside negative index materials *Appl. Phys. Lett.* **85** 2472–4
[34] Wilson J D and Schwartz Z D 2005 Multifocal flat lens with left-handed metamaterial *Appl. Phys. Lett.* **86** 021113
[35] Parimi P V, Lu T W, Vodo P and Sridhar S 2003 Imaging by flat lens using negative refraction *Nature* **426** 404
[36] Guven K, Aydin K, Alici B K, Soukoulis C M and Ozbay E 2004 Spectral negative refraction and point focusing analysis of a two-dimensional left-handed photonic crystal lens *Phys. Rev. B* **70** 205125
[37] Iyer A K, Kremer P C and Eleftheriades G V 2003 Experimental and theoretical verification of focusing in a large, periodically loaded transmission line negative refractive index metamaterial *Opt. Exp.* **11** 696–708
[38] Lu W T and Sridhar S 2005 Flat lens without optical axis: Theory of imaging *Opt. Exp.* **13** 10673–80
[39] Aydin K, Bulu I, and Ozbay E 2006 Verification of impedance matching at the surface of left-handed materials *Microwave Opt. Tech. Lett.* at press